Atomic Layer Deposition of Zirconium Titanium Oxide from Titanium Isopropoxide and Zirconium Chloride

Antti Rahtu,* Mikko Ritala, and Markku Leskelä

Department of Chemistry, University of Helsinki, P.O. Box 55, FIN-00014 Helsinki, Finland

Received October 23, 2000. Revised Manuscript Received January 31, 2001

Atomic layer deposition of $Zr_xTi_yO_z$ thin films using titanium isopropoxide and zirconium chloride as precursors in a temperature range of 200−300 °C was studied. Instead of using water or other compounds as a separate oxygen source, titanium isopropoxide served as both an oxygen and a metal source. At 300 °C the growth rate was 1.2 Å/cycle. The permittivity of the $Zr_xTi_yO_z$ films was 45−65, and the leakage current was 10^{-4} A/cm^2 at 0.2 MV/cm. The films were studied by means of spectrophotometry, X-ray diffraction, energy-dispersive X-ray spectroscopy, ion beam analysis, and electrical measurements.

Introduction

The dimensions of the microelectronic devices are shrinking fast according to Moore's law.[1] Soon we will be accessing device sizes where the materials used earlier are approaching their fundamental limits.[2−4] The key component of a modern microprocessor is a metal oxide semiconductor field effect transistor (MOSFET). The scaling of a MOSFET puts more and more demands especially on the properties of the gate oxide. So far the gate oxides have been based on silicon dioxide (SiO_2). The thickness of the SiO_2 gate oxide is projected to be scaled down to 1 nm around 2010.[2,4] This oxide thickness would correspond to about four atom layers of SiO_2. When the gate oxide is so thin, it does not work anymore as an insulator because the tunneling current through it is significant. An obvious solution to this problem is to use materials with a higher permittivity than SiO_2. Then it is possible to use a thicker oxide layer and still have the same unit area capacitance for the gate insulator:

$$C/A = \epsilon_0\epsilon_r/d \quad (1)$$

where ϵ_0 is the permittivity of the vacuum and ϵ_r is the relative permittivity of the insulator, A is the area of the capacitor, and d is the thickness of the insulator.

If the gate oxide is composed of more than one layer, each layer forms a capacitor in series with the other layers. Then the overall capacitance of the gate oxide stack can be obtained from

$$\frac{1}{C} = \sum\frac{1}{C_i} \quad (2)$$

where C_i is the capacitance of each capacitor in series.

Therefore, the high-permittivity material should be deposited on silicon in a way that only one or two atomic layers of SiO_2 are formed at the interface. With thicker SiO_2 layers, the effective capacitance of the capacitor becomes much lower than when only the high-permittivity material would be present. Interfacial SiO_2 may be formed by two mechanisms: (i) a reaction between silicon and high-permittivity oxide and (ii) oxidation of the silicon surface during the oxide deposition.[5] The first mechanism is avoided by choosing materials that are thermodynamically stable in contact with silicon. From this point of view, the most promising materials are zirconium dioxide (ZrO_2) and aluminum oxide (Al_2O_3).[6] The second mechanism is avoided when the silicon surface is not exposed to a strong oxidizer at the beginning of the growth of the high-permittivity material.

The uniformity of the gate oxide is a very important issue. Variations in the thickness and electrical properties of the films should be as small as possible. One interesting method for depositing ultrathin gate oxides is atomic layer deposition (ALD), also called atomic layer epitaxy (ALE).[7−12] ALD is based on sequential surface reactions which are accomplished by leading the reactant vapors into the reactor in a cyclic manner, one at a time, separated by purging periods. When the process conditions are properly chosen, all of the surface reactions are saturative, making the film growth self-limiting. This offers specific practical advantages, such

* To whom correspondence should be addressed. E-mail: antti.rahtu@helsinki.fi. Fax: +358-9-19150198.

(1) Moore, G. *Tech. Dig.—Int. Electron Devices Meet.* **1975**, 11.
(2) Semiconductor Industry Association, National Technology Road map for Semiconductors: Technology Needs (SEMATECH, Austin, TX, 1999). See also public.itrs.net/.
(3) Schulz, M. *Nature* **1999**, *399*, 729.
(4) Packan, P. A. *Science* **1999**, *285*, 2079.
(5) Ritala, M.; Kukli, K.; Rahtu, A.; Räisänen, P. I.; Leskelä, M.; Sajavaara, T.; Keinonen, J. *Science* **2000**, *288*, 319.
(6) Hubbard, K. J.; Schlom, D. G. *J. Mater. Res.* **1996**, *11*, 2757.
(7) Suntola, T.; Antson, J.; Pakkala, A.; Lindfors, S. *SID 80 Digest* **1980**, 108.
(8) Suntola, T.; Antson, J. U.S. Patent 4,058,430, 1977.
(9) Suntola, T. *Mater. Sci. Rep.* **1989**, *4*, 261.
(10) Suntola, T. Atomic Layer Epitaxy. *Handbook of Crystal Growth*; Elsevier: 1994; Vol. 3 (*Thin Films and Epitaxy, Part B: Growth Mechanisms and Dynamics*), Chapter 14.
(11) Niinistö, L.; Ritala, M.; Leskelä, M. *Mater. Sci. Eng.* **1996**, *B41*, 23.
(12) Leskelä, M.; Ritala, M. *J. Phys. IV* **1995**, *5*, C5-937.
(13) Ritala, M.; Leskelä, M.; Dekker, J.-P.; Mutsaers, C.; Soininen, P. J.; Skarp, J. *Chem. Vap. Deposition* **1999**, *5*, 7.
(14) Ritala, M. *Appl. Surf. Sci.* **1997**, *112*, 223.

10.1021/cm0012062 CCC: $20.00
Published on Web 04/03/2001

as excellent conformality, accurate and simple thickness control, and large area uniformity.[12−14]

Usually the oxygen source in ALD is water (H_2O), alcohol (ROH), nitrous oxide (N_2O), ozone (O_3), oxygen (O_2) or hydrogen peroxide (H_2O_2).[11] These oxygen sources can easily form a thin SiO_2 layer on the silicon surface during the growth. This layer can decrease the total capacitance of the gate oxide as discussed above. For example, when ZrO_2 is deposited from $ZrCl_4$ and water by ALD on HF-etched silicon, an interfacial silicon oxide or zirconium silicate layer is formed.[15,16] Recently, a new method for growing oxide thin films by ALD without strong oxidizers was introduced.[5,17] In this method a metal alkoxide serves as both the oxygen and metal source. With this novel method Al_2O_3 was deposited on silicon without an interfacial SiO_2 layer.[5] On the other hand, recent results[15,18] have shown that, by contrast to ZrO_2,[15,16] Al_2O_3 can be deposited on silicon without an interfacial SiO_2 layer also with the conventional ALD process using $Al(CH_3)_3$ and water as precursors.

ZrO_2 thin films are possible candidates for gate oxides.[19,20] ZrO_2 has many important properties such as a relatively high permittivity and a reasonably low leakage current. The permittivities for monoclinic and stabilized tetragonal ZrO_2 thin films were about 20[20,21] and 28−40,[22,23] respectively. The leakage current for monoclinic ZrO_2 was 5×10^{-6} A/cm^2 at 1.5 MV/cm.[20] ZrO_2 thin films have been grown by ALD from $ZrCl_4$ and water.[15,16,24,25] The chlorine content of the films was below 0.5 atomic %. The refractive index was 2.2 at the wavelength of 580 nm. Zirconium alkoxides have also been examined as precursors in ALD, but the main problem was the thermal instability.[26]

TiO_2 thin films grown by ALD have a high refractive index (n(580 nm) ≈ 2.6),[27−30] but they suffer from low resistivity which is apparently due to oxygen deficiency and is characteristic of TiO_2 films prepared also by other methods. TiO_2 thin films have been grown by ALD from $TiCl_4$,[27] TiI_4,[31,32] $Ti(OCH(CH_3)_2)_4$,[29] and $Ti(OC_2H_5)_4$.[30] The oxygen source has usually been water, but H_2O_2 has been used too. When the metal precursor was $Ti(OCH(CH_3)_2)_4$, the growth rate was 0.3 Å/cycle at the temperature range of 250−325 °C. At temperatures above 350 °C, the growth is no more self-limiting but occurs mainly by decomposition of $Ti(OCH(CH_3)_2)_4$. $Ti(OCH(CH_3)_2)_4$ decomposes also at lower temperatures but in lesser extents. At 250 °C the effect of thermal decomposition on the total growth rate is only about 3%.[29]

$ZrTiO_4$ thin films have been deposited with many different methods such as radio frequency[33−36] and direct-current magnetron sputtering[37] and sol−gel.[38,39] To our knowledge, no papers on chemical vapor deposition (CVD) or ALD of $ZrTiO_4$ thin films have been published. $ZrTiO_4$ thin films have a reasonably high permittivity of about 40 within a frequency range from kilohertz to a few gigahertz.[33,37] The temperature dependence of the permittivity is small, and the dielectric losses are also usually low (0.017−0.038 at 100 kHz).[37] Tin doping improves significantly the $ZrTiO_4$ film dc resistivity and breakdown characteristics, while having only a marginal effect on the permittivity.[33,40]

The purpose of this study is to grow $Zr_xTi_yO_z$ thin films by a water-free ALD process. The combination of TiO_2 and ZrO_2 is hoped to produce an insulator which has high permittivity and a reasonably low leakage current.

Experimental Section

Experiments were made in a hot-wall flow-type ALD F-120 reactor manufactured by ASM Microchemistry.[41] The pressure in the reactor during the growth was about 10 mbar. Nitrogen (99.9995%) obtained from a Schmidlin NG 3000 nitrogen generator was used as a carrier and purging gas. The films were grown on two 5 × 5 cm^2 bare and Al_2O_3-covered soda lime glass substrates that were located 2 mm apart from each other, forming a narrow flow channel in between. The substrates were cleaned ultrasonically in ethanol and distilled water before use. The substrates were blown dry with nitrogen. Some samples were deposited also on HF (1%)-etched p-type silicon. $ZrCl_4$ (Aldrich, 97%) and $Ti(OCH(CH_3)_2)_4$ (Aldrich, 97%) were used as precursors. The source temperatures were 170 and 40 °C, respectively. The reaction temperature was varied between 200 and 300 °C.

Film thicknesses and refractive indexes were determined by fitting measured reflectance or transmittance spectra with a Thin film program.[42] The spectra were measured in the range of 380−1100 nm by a Hitachi U-2000 spectrophotometer.

The crystallinity of the films was measured with a Bruker D8 Advance powder X-ray diffractometer (XRD) in grazing incidence mode with an angle of incidence of 1° using Cu Kα

(15) Gusev, E. P.; Copel, M.; Cartier, E.; Baumvol, I. J. R.; Krug, C.; Gribelyuk, M. A. *Appl. Phys. Lett.* **2000**, *76*, 176.
(16) Haukka, S.; Tuominen, M.; Granneman, E. *Semicon Europa/Semieducation* **2000**, in press.
(17) Kukli, K.; Ritala, M.; Leskelä, M. *Chem. Mater.* **2000**, *12*, 1914.
(18) Gusev, E. P.; Copel, M.; Cartier, E.; Buchanan, D.; Okorn-Schmidt, H.; Gribelyuk, M.; Falcon, D.; Murphy, R.; Molis, S.; Baumvol, I. J. R.; Krug, C.; Jussila, M.; Tuominen, M.; Haukka, S. *Proc. Electrochem. Soc.* **2000**, *2*, 477.
(19) Kattelus, H.; Ylilammi, M.; Salmi, J.; Ranta-aho, T.; Nykänen, E.; Suni, I. *Mater. Res. Soc. Symp. Proc.* **1993**, *284*, 511.
(20) Shappir, J.; Anis, A.; Pinsky, I. *IEEE Trans. Electron Devices* **1986**, *ED-33*, 442.
(21) Treichel, H.; Mitwalsky, A.; Tempel, G.; Zorn, G.; Bohling, D. A.; Coyle, K. R.; Felker, B. S.; George, M.; Kern, W.; Lane, A. P.; Sandler, N. P. *Adv. Mater. Opt. Electron.* **1995**, *5*, 163.
(22) Thompson, D. P.; Dickins, A. M.; Thorp, J. S. *J. Mater. Sci.* **1992**, *27*, 2267.
(23) Subramania, M. A.; Shannon, R. D. *Mater. Res. Bull.* **1989**, *24*, 1477.
(24) Ritala, M. *Ann. Acad. Sci. Fenn., Ser. A2* **1994**, *257*, 1.
(25) Ritala, M.; Leskelä, M. *Appl. Surf. Sci.* **1994**, *75*, 333.
(26) Kukli, K.; Ritala, M.; Leskelä, M. *Chem. Vap. Deposition* **2000**, *6*, 297.
(27) Ritala, M.; Leskelä, M.; Nykänen, E.; Soininen, P.; Niinistö, L. *Thin Solid Films* **1993**, *225*, 288.
(28) Aarik, J.; Aidla, A.; Kiisler, A.-A.; Uustare, T.; Sammelselg, V. *Thin Solid Films* **1997**, *305*, 270.
(29) Ritala, M.; Leskelä, M.; Niinistö, L.; Haussalo, P. *Chem. Mater.* **1993**, *5*, 1174.
(30) Ritala, M.; Leskelä, M.; Rauhala, E. *Chem. Mater.* **1994**, *6*, 556.
(31) Kukli, K.; Ritala, M.; Schuisky, M.; Leskelä, M.; Sajavaara, T.; Keinonen, J.; Uustare, T.; Hårsta, A. *Chem. Vap. Deposition* **2000**, *6*, 303.
(32) Kukli, K.; Aidla, A.; Aarik, J.; Schuisky, M.; Hårsta, A.; Ritala, M.; Leskelä, M. *Langmuir* **2000**, *16*, 8122.
(33) Ramakrishnan, E. S.; Cornett, K. D.; Shapiro, G. H.; Howng, W.-Y. *J. Electrochem. Soc.* **1998**, *145*, 358.
(34) Chang, D.-A.; Lin, P.; Tseng, T.-Y. *J. Appl. Phys.* **1995**, *78*, 7103.
(35) Chang, D.-A.; Lin, P.; Tseng, T.-Y. *J. Appl. Phys.* **1995**, *77*, 4445.
(36) Chang, D.-A.; Lin, P.; Tseng, T.-Y. *Appl. Phys. Lett.* **1994**, *64*, 3252.
(37) Kim, T.; Oh, J.; Park, B.; Hong, K. S. *Appl. Phys. Lett.* **2000**, *76*, 3043.
(38) Miller, J. M.; Lakshmi, L. J. *J. Phys, Chem. B* **1998**, *102*, 6465.
(39) Merkle, R.; Bertagnolli, H. *J. Mater. Chem.* **1998**, *8*, 2433.
(40) Nakagawara, O.; Toyota, Y.; Kobayashi, M.; Yoshino, Y.; Katayama, Y.; Tabata, H.; Kawai, T. *J. Appl. Phys.* **1996**, *80*, 388.
(41) Suntola, T. *Thin Solid Films* **1992**, *216*, 84.
(42) Ylilammi, M.; Ranta-aho, T. *Thin Solid Films* **1993**, *232*, 56.

radiation. The chemical composition of the films was examined by a Link ISIS energy-dispersive X-ray spectrometer (EDX) with an acceleration voltage of 20 kV. The composition depth profiling of the films was carried out by ion beam analysis utilizing time-of-flight elastic recoil detection analysis (TOF-ERDA) using a 34 MeV I^{6+} ion beam produced by a 5 MV EPG-10-II tandem accelerator.[43,44] The detection limit was about 0.1 atomic %. The depth resolution was 10−15 nm in the surface and 50 nm in the interface between the film and substrate. The elements in this study had such different atomic weights that there was no problem distinguishing them. The sample degradation was not a problem with the films analyzed in this study. Hydrogen was also analyzed with the same experimental setup, but because the sensitivity of the flight time port is not the same for hydrogen as it is for other elements, the values were corrected using previously measured correction values. A more detailed description of the TOF-ERDA method is given in ref 44.

To measure the electrical properties of the films, soda lime glasses covered with an Al_2O_3 ion barrier layer and patterned In_2O_3:Sn (ITO) electrodes were used as substrates. An array of evaporated aluminum was used as the upper electrodes. The effective area of a single electrode was 12 mm^2. The films were not heat-treated after the deposition. Some samples were deposited also on silicon and measured from a Pt−oxide−Si−Al capacitor structure where platinum is the top electrode and aluminum the backmetallization of the silicon wafer. This structure was heat-treated at 300 °C for 30 min in nitrogen in order to improve the adhesion of the platinum electrodes. The heat treatment temperature was the same as the growth temperature, and therefore it should not effect the electrical properties of the oxide. The capacitances were measured using a HP4275A LCR meter. Current−voltage characteristics were recorded using a Keithley 2400 source meter. The electrical measurements were carried out at room temperature.

Results and Discussion

The reactions between metal halides and alkoxides into oxides and alkyl halides are known from nonhydrolytic sol−gel processes.[45,46] Similarly, the overall reaction in ALD of $ZrTiO_4$ from $Ti(OCH(CH_3)_2)_4$ and $ZrCl_4$ can be suggested:

$$Ti(OCH(CH_3)_2)_4(g) + ZrCl_4(g) \rightarrow ZrTiO_4(s) + 4(CH_3)_2CHCl(g) \quad (3)$$

At 200 °C no film growth occurred. At 250 °C the growth rate was constant and the refractive index of the films was in the range of 2.27−2.35 when the Ti-$(OCH(CH_3)_2)_4$ pulse length was longer than 0.5 s (Figure 1). The refractive index is quite close to the bulk values of $ZrTiO_4$ (n(550) = 2.37).[47] The values obtained from thin films were slightly smaller (n(550) = 2.22−2.37).[34,35] The $Zr_xTi_yO_z$ films were more uniform when they were grown on the Al_2O_3-coated glass substrates as compared to the bare soda lime glass substrates. Therefore, most of the films were grown on the Al_2O_3-coated substrates.

When the $ZrCl_4$ pulse length was 0.2 s, the films were more uniform than with longer $ZrCl_4$ pulses and thus the $ZrCl_4$ pulse length should be kept as short as possible. With short (0.2 s) $ZrCl_4$ pulses, the thickness variation over the substrates was only about 5%. The thickness uniformity is comparable to the TiO_2[29,30] and ZrO_2[25] films grown by the conventional ALD processes using water as the oxygen source.

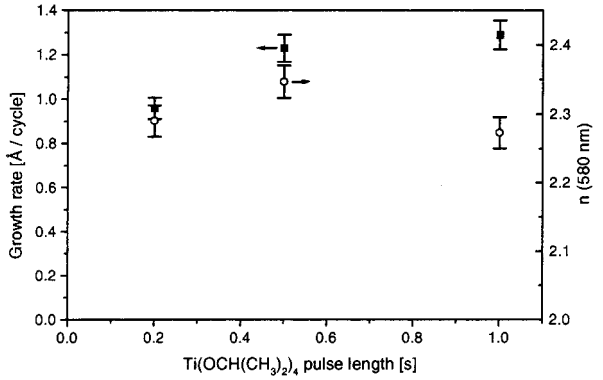

Figure 1. Effect of the $Ti(OCH(CH_3)_2)_4$ pulse length at 250 °C on the growth rate (boxes) and refractive indexes (circles). The films were grown on bare soda lime glass. The $ZrCl_4$ pulse time was 1.0 s, and the purge time was 0.5 s.

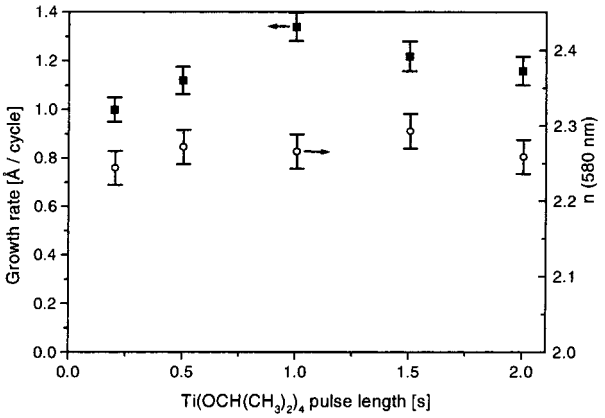

Figure 2. Effect of the $Ti(OCH(CH_3)_2)_4$ pulse length at 300 °C on the growth rate (boxes) and refractive indexes (circles). The films were grown on Al_2O_3-coated glass. The $ZrCl_4$ pulse length was 0.2 s, and the purge time was 0.5 s.

According to the EDX measurements, the chlorine content of the films deposited at 250 °C was quite high over 9 atomic % and was not affected by the Ti(OCH-$(CH_3)_2)_4$ pulse length. This suggests that this temperature is too low to complete the surface reactions.

At 300 °C the growth rates and refractive indexes of the films were constant when the $Ti(OCH(CH_3)_2)_4$ pulse length was above 1.0 s (Figure 2). According to the EDX measurements, all of the films had a uniform Zr/(Zr + Ti) ratio and chlorine content when the $Ti(OCH(CH_3)_2)_4$ pulse length was above 0.2 s. The exact metal ratios were determined with TOF-ERDA, and they were 0.62 and 0.58 with $Ti(OCH(CH_3)_2)_4$ pulse lengths of 0.2 and 1.0 s, respectively (Figure 3). This ratio is higher than that (Zr/(Zr + Ti) = 0.50) which would be obtained if the film would grow strictly according to reaction (3). $ZrCl_4$ is a very reactive precursor, so it is possible that zirconium replaces titanium during the $ZrCl_4$ pulse according to the thermodynamically possible exchange reaction

$$ZrCl_4(g) + TiO_2(s) \rightarrow ZrO_2(s) + TiCl_4(g); \quad \Delta G(300\ °C) = -4.8\ kJ/mol \quad (4)$$

(43) Jokinen, J.; Haussalo, P.; Keinonen, J.; Ritala, M.; Riihelä, D.; Leskelä, M. *Thin Solid Films* **1996**, *289*, 159.
(44) Jokinen, J.; Keinonen, J.; Tikkanen, P.; Ahlgren, T.; Nordlund, K. *Nucl. Instrum. Methods Phys. Res.* **1996**, *B119*, 533.
(45) Corriu, R. J. P.; Leclercq, D.; Lefèvre, P.; Mutin, P. H.; Vioux, A. *J. Mater. Chem.* **1992**, *2*, 673.
(46) Vioux, A. *Chem. Mater.* **1997**, *9*, 2292.
(47) Coughanour, L. W.; Roth, R. S.; DeProsse, V. A. *J. Res. Natl. Bur. Stand.* **1954**, *52*, 2470.

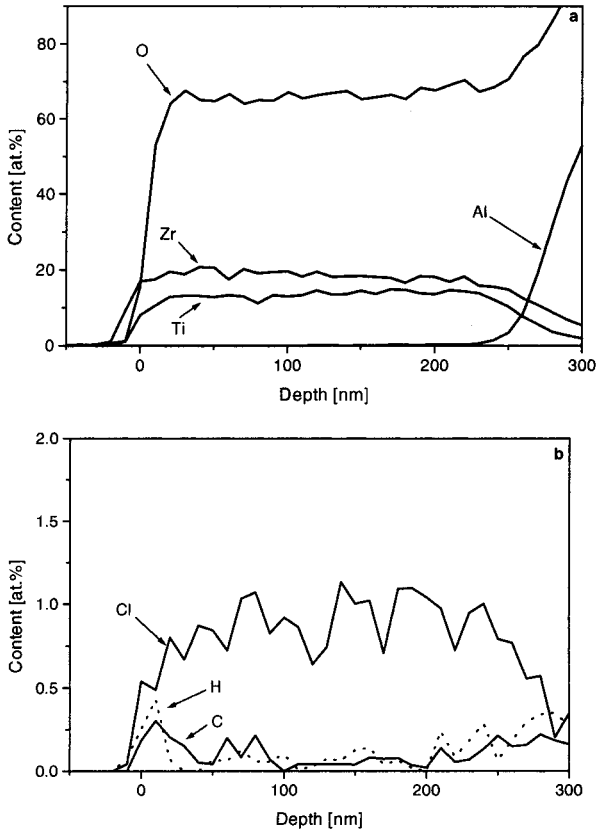

Figure 3. Depth profiles of (a) the main components and (b) impurities as measured by TOF-ERDA. The films were grown on top of Al_2O_3-coated glass at 300 °C. The film thickness was 268 nm. The $Ti(OCH(CH_3)_2)_4$ and $ZrCl_4$ pulse lengths were 1.0 and 0.2 s, respectively.

The depth profiling of the films showed that the metal and oxygen contents were constant through the whole film thickness (Figure 3). The carbon and hydrogen impurity contents were small, below 0.5 atomic %, in the films grown at 300 °C (Figure 3b). The carbon and hydrogen impurity contents were higher at the surface, but this is most probably due to a contamination of the film surface after the growth. When the $Ti(OCH(CH_3)_2)_4$ pulse length was increased from 0.2 to 1.0 s, the chloride content decreased from 1.0 to 0.2 atomic %. However, this had no effect on the Zr/(Zr + Ti) ratio. The chloride content of the ZrO_2 films grown from water and $ZrCl_4$[24,25] was below the detection limit of Rutherford backscattering spectrometry (RBS) measurement, i.e., in that study below 0.5 atomic %.

When the optically measured physical film thickness and the areal density of atoms measured with TOF-ERDA are combined, a density of about 4.7 g/cm^3 was estimated for the films. The density is between that of TiO_2 (anatase, 3.84 g/cm^3) and ZrO_2 (monoclinic, 5.6 g/cm^3).[48] The density of the orthorhombic $ZrTiO_4$ is 5.1 g/cm^3.[49]

According to the XRD measurements, the $Zr_xTi_yO_z$ films were amorphous when grown at 250 °C. The films made at 300 °C were slightly crystallized (Figure 4). According to the peak positions, the crystalline phase was the orthorhombic $ZrTiO_4$.[49] In addition, there was a small shoulder at 25.2 °C which could be due to a small amount of TiO_2 (anatase). For the gate oxide applications, amorphous films are usually preferred because in crystalline films grain boundaries increase the leakage current and the probability for electrical breakdown.

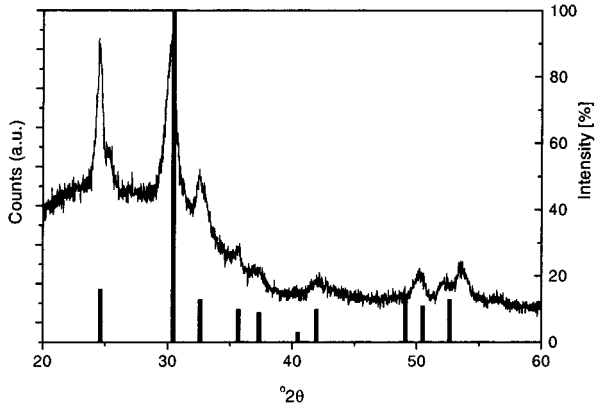

Figure 4. XRD patterns of $Zr_xTi_yO_z$ films grown at 300 °C. The $Ti(OCH(CH_3)_2)_4$ and $ZrCl_4$ pulse lengths were 1.0 and 0.2 s, respectively. For comparison, the positions and relative intensities of the reflections given for the reference $ZrTiO_4$[49] are marked with bars.

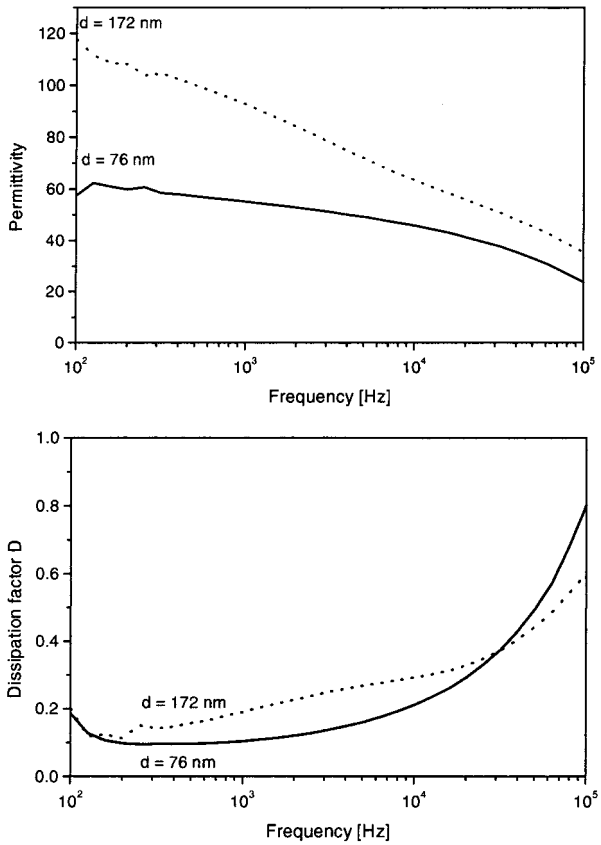

Figure 5. Frequency dependence of the permittivity and dissipation factor of $ZrTiO_4$ films grown at 300 °C. The sign of the electric field expresses the voltage applied to the Al electrodes in the ITO−oxide−Al capacitor structures.

The permittivities of the films, measured in the ITO−oxide−Al capacitors, were rather high (ϵ_r = 45−65 at 10 kHz) but decreased as a function of frequency (Figure

(48) *CRC Handbook of Chemistry and Physics*, 73rd ed.; CRC Press: Boca Raton, FL, 1992−1993; pp 4−108 and 4−113.
(49) Joint Committee on Powder Diffraction Standards, Card 34-0415, JCPDS, International Center for Diffraction Data, Newton Square, PA.
(50) Joshi, P. C.; Desu, S. B. *J. Appl. Phys.* **1996**, *80*, 2349.
(51) Feldman, C. *J. Appl. Phys.* **1989**, *65*, 872.

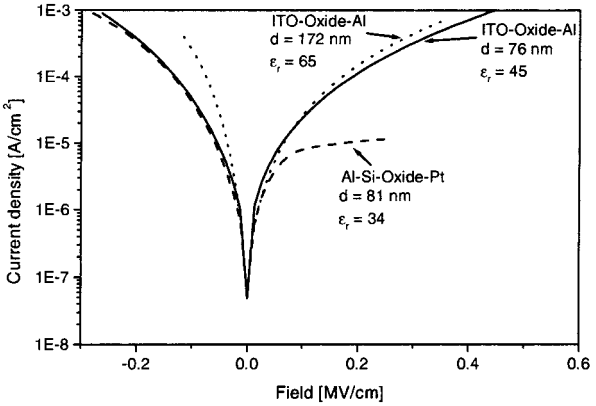

Figure 6. Leakage current density versus electric field of the $ZrTiO_4$ films grown at 300 °C. The sign of electric field expresses the voltage applied to the Al and Pt top electrodes in the ITO−oxide−Al and Al−Si−oxide−Pt capacitor structures. The calculated permittivity values are given also.

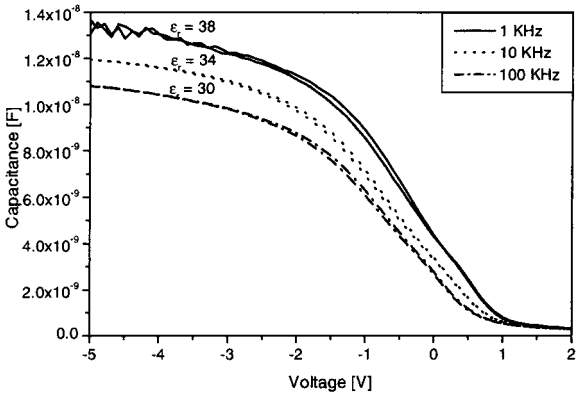

Figure 7. Capacitance versus voltage curves of $ZrTiO_4$ films grown at 300 °C. The sign of the electric field expresses the voltage applied to Pt electrodes in the Al−Si−oxide−Pt capacitor structures. The voltage was scanned from negative to positive and back.

5a). The permittivity was higher in the thicker film. Therefore, it seems that the growth is started with a less crystalline layer and later more crystalline material develops. This thickness dependence has been observed for $ZrTiO_4$ earlier in both metal−insulator−metal (MIM) and metal−insulator−silicon (MIS) structures.[33] In the MIS structure, the permittivity showed a quite strong dependence on the $ZrTiO_4$ thickness, which was suggested to be mostly due to a SiO_2 interface layer.[33] Also in the MIM structure, the permittivity decreased when the film thickness was below 100 nm, but to a lesser extent.[33] Similar connections between the dielectric layer thickness and electrical properties have been observed also for other materials.[50,51]

Another important parameter of the capacitor is the dissipation factor D:

$$D = 1/2\pi fCR \qquad (5)$$

where f is the frequency, C is the capacitance, and R is the parallel film resistance. The value of D increases with the conductance of the capacitor material, being thus directly related to the dielectric losses. The D value was rather high and increased from 0.1 to 0.5 as the frequency was increased from 100 Hz to 50 kHz (Figure 5b). When the frequency was still increased, the permittivity decreased and the dissipation factor increased. This is most probably due to a resonance frequency which is caused by the intrinsic frequency dependence of the material, any interfacial barrier, or the effects due to electrodes and wires. This same effect has been observed earlier in $ZrTiO_4$[37] and $Bi_4Ti_3O_{12}$[50] thin films, for example. As is typical for the high-permittivity materials, which have relatively small band gaps and often also show a tendency toward oxygen deficiency, the dc leakage currents were also here quite high (Figure 6). In MOSFET high leakage currents increase power consumption and generate heat, which can deteriorate the device. When the oxide was grown on silicon, it had a lower permittivity ($\epsilon_r = 34$ at 10 kHz), but the frequency dependence was also decreased (Figure 7). The hysteresis in the $C-V$ curve was also quite small (Figure 7).

One possibility for the permittivity difference between the $Zr_xTi_yO_z$ films grown on silicon and ITO could be that a low-permittivity layer is formed on silicon during the growth. If this layer was SiO_2, the observed decrease in the total capacitance on silicon as compared with ITO would correspond to a 2.5 nm thick SiO_2 layer which appears rather thick. More probably an amorphous low-permittivity $Zr_xSi_yO_z$ layer is formed at the interface between the oxide and silicon. This layer itself has a lower permittivity than $Zr_xTi_yO_z$ and therefore reduces the total capacitance. Furthermore, this amorphous layer can also reduce the crystallinity and therefore also the permittivity of the $Zr_xTi_yO_z$ growing on top of it.

Conclusions

The ALD of $Zr_xTi_yO_z$ using titanium isopropoxide and zirconium chloride as precursors was carried out. At 250 °C the chloride content was high, above 9 atomic %. The upper limit for this process is 350 °C, where the $Ti(OCH(CH_3)_2)_4$ precursor starts to decompose extensively, affecting the film properties. Therefore, the most suitable growth temperature is around 300 °C. At 300 °C the growth rate was 1.2 Å/cycle. The carbon and hydrogen contents were below 0.5 atomic %. The films contained 0.2−1 atomic % chlorine. The films grown at 250 °C were amorphous, but those made at 300 °C were partially crystallized. The permittivity of the films grown on ITO at 300 °C was rather high ($\epsilon_r = 45-65$ at 10 kHz), but the leakage current was also high (10^{-4} A/cm^2 at 0.2 MV/cm). The permittivity of the film grown on silicon was somewhat lower ($\epsilon_r = 35$ at 10 kHz).

Acknowledgment. The authors are thankful to Mr. Marko Vehkamäki for performing the EDX measurements and Mr. Timo Sajavaara for the TOF-ERDA measurements. The authors appreciate the opportunity to carry out the EDX analysis at the Electron Microscopy Unit at University of Helsinki. This work has been supported by the Academy of Finland and the Finnish National Technology Agency (TEKES), Helsinki, Finland.

CM0012062